ARTICLE

Population pharmacokinetic analysis identifies an absorption process model for mycophenolic acid in patients with renal transplant

Yuki Suzuki[1] | Noriko Matsunaga[2] | Takahiko Aoyama[1] | Chika Ogami[3] | Chihiro Hasegawa[1] | Satofumi Iida[1,4] | Hideto To[3] | Takashi Kitahara[5] | Yasuhiro Tsuji[1]

[1]Laboratory of Clinical Pharmacometrics, School of Pharmacy, Nihon University, Funabashi, Chiba, Japan

[2]Department of Hospital Pharmacy, Nagasaki University Hospital, Nagasaki, Nagasaki, Japan

[3]Department of Medical Pharmaceutics, School of Pharmacy and Pharmaceutical Sciences, University of Toyama, Toyama, Toyama, Japan

[4]Department of Clinical Pharmacology, Yokohama University of Pharmacy, Yokohama, Kanagawa, Japan

[5]Department of Clinical Pharmacology, Graduate School of Medicine, Yamaguchi University, Ube, Yamaguchi, Japan

Correspondence
Yasuhiro Tsuji, Laboratory of Clinical Pharmacometrics, School of Pharmacy, Nihon University, 7-7-1 Narashinodai, Funabashi, Chiba, 274-8555, Japan.
Email: tsuji.yasuhiro@nihon-u.ac.jp

Abstract

The pharmacokinetics (PKs) of mycophenolic acid (MPA) exhibit considerable complexity and large variability. We developed a population pharmacokinetic (popPK) model to predict the complex PK of MPA by examining an absorption model. Forty-two patients who had undergone renal transplantation were included in this study. popPK analysis, incorporating several absorption models, was performed using the nonlinear mixed-effects modeling program NONMEM. The MPA area under the concentration-time curve at 0–12 h (AUC0–12) was simulated using the final model to calculate the recommended dose. The PK of MPA was adequately described using a two-compartment model incorporating sequential zero- and first-order absorption with lag time. Total body weight, renal function (RF), and posttransplantation day (PTD) were included as covariates affecting MPA PK. The final model estimates were 7.56, 11.6 L/h, 104.0 L, 17.3 L/h, 169.0 L, 0.0453, 0.283, and 1.95 h for apparent nonrenal clearance, apparent renal clearance, apparent central volume of distribution, apparent intercompartmental clearance, apparent peripheral volume of distribution, absorption half-life, lag time, and duration of zero-order absorption, respectively. Simulation results showed that a dose regimen of 500–1000 mg twice daily is recommended during the early posttransplantation period. However, dose reduction could be required with increased PTD and decreased RF. The complex PK of MPA was explained using an absorption model. The developed popPK model can provide useful information regarding individual dosing regimens based on PTD and RF.

Study Highlights

WHAT IS THE CURRENT KNOWLEDGE ON THE TOPIC?

Mycophenolic acid (MPA) exposure is used as an index of the clinical outcomes of MPA. Population pharmacokinetic (PopPK) models incorporating absorption

and enterohepatic circulation (EHC) have been developed to describe the variable pharmacokinetics (PKs) of MPA.

WHAT QUESTION DID THIS STUDY ADDRESS?

Despite some studies suggesting that incorporating popPK model with EHC does not improve model fitting, question remains whether EHC sufficiently explains the PK of MPA. This study aimed to develop a popPK model to predict the PK of MPA by comparing the absorption and EHC models.

WHAT DOES THIS STUDY ADD TO OUR KNOWLEDGE?

An EHC model was not selected in this study. Instead, a two-compartment model, incorporating sequential zero- and first-order absorption with lag time, was selected to describe the PK of MPA. Total body weight, renal function (RF), and posttransplantation day (PTD) were included as covariates affecting MPA PK. The simulation results indicated that achieving the target AUC0–12 requires reducing the mycophenolate mofetil dose with an increase in PTD and a decreased RF.

HOW MIGHT THIS CHANGE CLINICAL PHARMACOLOGY OR TRANSLATIONAL SCIENCE?

The developed popPK model can be used to propose individual dosing regimens for patients undergoing renal transplantation based on PTD and RF.

INTRODUCTION

Mycophenolate mofetil (MMF) is an immunosuppressant widely used in kidney and other organ transplantation.[1–3] Following oral administration, MMF is rapidly hydrolyzed to its active metabolite, mycophenolic acid (MPA).[1,4] MPA is then metabolized in the liver to its pharmacologically inactive form, mycophenolic acid glucuronide (MPAG), which is mainly excreted in urine.[4] The remaining MPAG is excreted in bile, converted back to MPA by the gut flora, and subsequently reabsorbed (enterohepatic circulation, EHC).[1]

MPA exposure is used as an index of the clinical outcomes of MPA. A target MPA area under the concentration-time curve from 0 to 12h (AUC0–12) of 30–60mg h/L is recommended for effective treatment in patients with kidney transplant.[3,5] When the AUC0–12 falls outside the target range, the risks of graft rejection, leukopenia, and infection increase.[6,7] Nevertheless, the pharmacokinetic (PK) of MPA demonstrates large variability.[1] In addition to a typical single peak, an absorption delay or a second peak due to EHC is observed in some patients.[8,9] The PK of MPA is affected by several factors, such as renal function (RF), serum albumin level, genetic polymorphisms, posttransplantation day (PTD), and concomitant medications.[1] A better prediction of the PK of MPA is necessary to propose individualized dosing and improve clinical outcomes.

A population pharmacokinetic (PopPK) analysis is an approach for predicting the variable PK of MPA and estimating the individualized MPA AUC0–12. To date, popPK

models of MPA have been reviewed and summarized in several studies.[10,11] To describe the complex PK of MPA, various absorption and EHC models have been incorporated into the popPK model. As a popPK model examining the absorption process, a zero-order absorption model,[12,13] parallel zero- and first-order absorption model,[14] parallel first-order absorption model,[15] and transit compartment absorption model[16–18] have been reported. The EHC process has been incorporated into several popPK models of MPA to enhance accuracy.[15,16,19–23] However, a popPK model with an EHC process does not necessarily improve model fitting.[18,24,25] This raises question about the accuracy of the EHC process in explaining the PK of MPA.[26]

Therefore, we hypothesized that the PK of MPA could be explained by examining an absorption model, rather than an EHC model, using popPK model analysis. The objective of this study was to develop a popPK model to predict the PK of MPA by comparing the absorption and EHC models. Additionally, this study aimed to propose individualized dosing recommendations based on the PK of MPA using the predictions of the developed popPK model.

METHODS

Ethics

The study was performed in accordance with the guidelines outlined in the Declaration of Helsinki, following approval by the Ethical Review Boards of Nagasaki

University Hospital (approval number: 14052645-13) and Nihon University (School of Pharmacy, approval number: 19-018). Written informed consent was obtained from all individual patients.

Patients and data sources

Patients undergoing kidney transplant who received MMF (CellCept®; Chugai Pharmaceutical Group, Tokyo, Japan) at Nagasaki University Hospital between April 2011 and September 2019 were included in this analysis. Clinical data, including plasma MPA concentrations, were collected. The creatine values were determined by the enzymatic method, and creatinine clearance (CLcr) was calculated using the Cockcroft–Gault equation.[27] MMF (500–1000 mg) was administered twice daily, and steady-state blood samples were collected.

Determination of MPA concentrations

Two milliliters of blood was collected and centrifuged at 3000 rpm for 5 min to prepare plasma samples. Plasma MPA concentrations were measured using Dimension Xpand (Siemens, Germany) with a homogeneous particle-enhanced turbidimetric inhibition immunoassay (PETINIA) technique and MPA Flex reagent cartridge (Siemens). Plasma samples were analyzed within the stability period described in the manual of the MPA Flex reagent cartridge (8 h at room temperature, 14 days at 2–8°C, and 18 months at −20°C). A 200 μL plasma sample was used to measure MPA concentration. A standard solution of MPA was used, and the inter-day coefficient of variation (CV) of the inter-day precision sample containing 2.06, 6.68, 10.82, and 21.81 mg/L of MPA was <7%. The lower limit of quantification (LLOQ) was 0.2 mg/L, and the lower limit of detection was 0.12 mg/L. The calibration curve was linear over a concentration range of 0.2–30 mg/L for total MPA. The cross-reactivity was 0.6% when MPAG was 1000 μg/mL and MPA was 5.0 μg/mL.

PopPK

PopPK analysis was performed using the nonlinear mixed-effects modeling program NONMEM version 7.5.1 (ICON Development Solution, Ellicott City, MD, USA). First-order conditional estimation with the interaction method was used to estimate parameters and variability during the model-building process. PK modeling, visual predictive checks, bootstrapping, and simulations were performed using Wings for NONMEM (Nick Holford,

University of Auckland, New Zealand). Statistical analyses of the results were performed using R version 4.1.3 (R Foundation, Vienna, Austria).

For the base model, one-compartment, two-compartment, and three-compartment models with first-order absorption and elimination were assessed. Between-subject variability (BSV) in the MPA PK parameters was assessed using an exponential error model. Residual, unidentified variability was assessed using a combined proportional and additive error model. During model development, the units of MMF doses were normalized to account for their molecular weight ratios with MPA (MMF and MPA: 433.5 and 320.3 g/mol, respectively; https://pubchem.ncbi.nlm.nih.gov/). The initial estimates of each model were chosen based on values from previous publications and values obtained during the model development process (e.g., $CL/F = 14.3$, $V/F = 113$). In the popPK model incorporating the EHC process, the gallbladder compartment is connected to the central and gut compartments. The fraction of the central compartment to the gallbladder compartment (FGB) and gallbladder elimination half-life were parameterized. The start and duration of gallbladder emptying time after meals were estimated using a model event time (MTIME) set at 8 a.m., 12 p.m., and 6 p.m. as a meal time.[28]

To describe the absorption process, zero-order, first-order, sequential zero- and first-order, parallel zero- and first-order, parallel first-order, and transit compartment absorptions were tested. The absorption lag time was also evaluated. For transit compartment absorption, a model with a fixed number of transit compartments (the Erlang model)[29] and a model estimating the number of transit compartments (the Savic model)[30] were assessed. In the Erlang model, the transfer rate constant (ktr) for each transit compartment was the same. The number of parameters in the Erlang model was not changed in different number of transit compartments. In the Savic model, the range of transit compartment numbers was set to 0 or more.

Covariate model

The factor of size (F_{SIZE}) was employed to standardize PK parameters. Following the equation below, the allometric exponent (PWR) of F_{SIZE} was fixed at 0.75 for CL/F (and Q/F) and at 1 for VC/F (and VP/F).[31,32]

$$F_{SIZE} = \left(\frac{NFM}{NFM_{STD}} \right)^{PWR} \tag{1}$$

The Log$P$ of MPA is 2.8 (https://pubchem.ncbi.nlm.nih.gov/), suggesting that MPA is a lipophilic compound. Considering its distribution in fat mass, normal fat mass

(NFM) was incorporated. NFM was used as an index of body size.[31,32] The NFM of each individual patient was determined from total body weight (TBW), fat-free mass (FFM), fat mass (FAT), and the factor describing the influence of fat mass (F_{fat}) using the following equations: F_{fat} was included in the model and estimated.

$$NFM = FFM + F_{fat} \times FAT$$

$$FAT = TBW - FFM \quad (2)$$

The FFM was calculated from maximal weight height squared (WHS_{max}), WHS_{50}, and height (H) using Equation (3): WHS_{max} is the maximum FFM for any given H and WHS_{50} is the TBW value when FFM is half of WHS_{max}. WHS_{max} is 42.92 and 37.99 kg/m^2 and WHS_{50} is 30.93 and 35.98 kg/m^2 for males and females, respectively.[31,32]

$$FFM = WHS_{max} \times H^2 \times \left(\frac{TBW}{(WHS_{50} \times H^2 + TBW)} \right) (3)$$

The standard value of NFM (NFM_{std}) was calculated with a standard FFM value (56.1 kg) calculated from a standard TBW (70 kg) and a standard H (1.76 m).[33]

RF, defined as the ratio of the observed CLcr to the standard CLcr ($CLcr_{std}$),[33,34] was investigated as a covariate of clearance. CLcr was determined using the Cockcroft–Gault formula standardized to a TBW of 70 kg.[27] The RF was normalized to a standard CLcr ($CLcr_{std}$) of 6 L/h/70 kg (100 mL/min/70 kg) using Equation (4):

$$RF = \frac{CLcr}{CLcr_{std}} \quad (4)$$

It was hypothesized that apparent total clearance (CL_{total}/F) comprised both apparent nonrenal clearance ($CL_{nonrenal}/F$) and apparent renal clearance (CL_{renal}/F), with CL_{renal}/F being linearly related to RF. RF was incorporated into the model using a combination of $CL_{nonrenal}/F$ and CL_{renal}/F using the following equation:

$$CL_{total}/F = CL_{non-renal}/F + CL_{renal}/F \times RF \quad (5)$$

The PTD was investigated as a covariate for PK parameters. The PTD (F_{PTD}) was included in the model using Equation (6): PTD_{max} represented the maximum PTD considered in the analysis (84 days). The K_{PTD} is a factor that describes the effect of PTD. The F_{PTD} was included in apparent clearance (CL/F), apparent central volume of distribution (VC/F), absorption half-life (TABS), duration of zero-order absorption (D1), lag time (TLAG), and relative bioavailability (F1).

$$F_{PTD} = e^{K_{PTD} \times \frac{PTD}{PTD_{max}}} \quad (6)$$

Model evaluation and validation

The models were evaluated using the likelihood ratio test. The objective function value (OFV) was compared between the models using the chi-square test. A decrease in OFV (ΔOFV) exceeding the specified criteria (i.e., ΔOFV 3.84, degree of freedom = 1, $p = 0.05$, ΔOFV 6.63, degree of freedom = 1, $p = 0.01$) indicated a significant improvement.

Goodness-of-fit (GOF) plots were created to evaluate the model. The observed concentrations versus population-predicted concentrations (PRED), observed concentrations versus individual-predicted concentrations (IPRED), conditional weighted residuals (CWRESs) versus PRED, and CWRES versus time after dosing were evaluated.

The bootstrap method was used to assess the internal validity and robustness of the parameters (200 bootstrap samples). Initially, bootstrap samples were generated by random resampling of the original dataset. Parameters were estimated for each bootstrap sample. The mean, median, 95% confidence intervals, and relative standard errors of the parameters obtained from the 200 bootstrap replicates and the final estimated parameters from the original dataset were evaluated.

The predictive performance was assessed using a prediction-corrected visual predictive check (pcVPC). The observed concentrations were plotted against the median, 90 percentile intervals, and their 95% confidence intervals derived from the simulated concentrations using the final parameters ($n = 200$).

Simulation

The AUC0–12 of MPA was simulated for up to 90 days posttransplantation based on the final population PK model ($n = 1000$). AUC0–12 was calculated using the following equation:

$$AUC0 - 12 = F1 \times \frac{Dose}{CL_{total}/F} \quad (7)$$

The simulated dosing regimens included 250, 500, 750, and 1000 mg of MMF every 12 h based on a fixed standard TBW of 70 kg. The CLcr in patients with standard RF was assumed to be 100 mL/min/70 kg, while the CLcr in patients with renal impairment was assumed to be 25, 50, and 75 mL/min/70 kg. The target exposure (AUC0–12) for MPA was set at 30–60 mg h/L.[3,5] The percentage of patients within the target AUC0–12 was calculated, and the dosage that achieved the highest percentage was selected as the recommended dose.

TABLE 1 Baseline demographic and clinical data of the study participants.

	Unit	Number of participants	Observation interval		
			2.5%	50%	97.5%
Sex (male/female)	–	29/13	–	–	–
MMF dose (500 mg/750 mg/1000 mg)	–	10/25/7	–	–	–
Age	year	42	29.0	51.0	68.9
Height	m	42	1.50	1.66	1.80
Total body weight	kg	42	39.6	55.9	77.5
Posttransplantation day	days	42	23	40	84
Albumin	g/dL	42	2.7	3.7	4.4
Alanine aminotransferase	IU/L	42	5.0	14.0	163.7
Aspartate aminotransferase	IU/L	42	7.0	12.0	63.9
Serum creatinine	mg/dL	42	0.5	1.6	14.3
Creatinine clearance	mL/min/70 kg	42	6.6	52.8	148.8
Blood urea nitrogen	mL/min	42	11.0	26.0	95.9
Tacrolimus concentration	µg/L	24	2.0	6.9	14.7
Prednisone dose	mg/day	23	0.0	10.0	50.0

RESULTS

Patients′ background

Forty-two patients with renal transplants who received MMF were included. The demographic and clinical characteristics of the patients are summarized in Table 1. The baseline dose of MMF was 500 mg ($n = 10$), 750 mg ($n = 25$), and 1000 mg ($n = 7$), administered twice daily, every 12 h.

PopPK of MPA

The popPK model of MPA was developed based on 312 MPA observations collected from 14 days pretransplantation to 84 days posttransplantation (Figure 1). All MPA concentrations were above the LLOQ, with none falling below this threshold. The OFV of the two-compartment model exhibited a significant decrease compared with that of the one-compartment model (ΔOFV 17.81, degrees of freedom 2, $p < 0.01$). However, the OFV of the three-compartment model did not show significant improvement. Therefore, the two-compartment model was selected as the preliminary structural model. Additionally, incorporating an EHC process did not significantly improve the OFV.

A summary of the various absorption models investigated is presented in Table S1 and Figure S1. The OFV of the sequential zero- and first-order absorption model was the lowest. A two-compartment model,
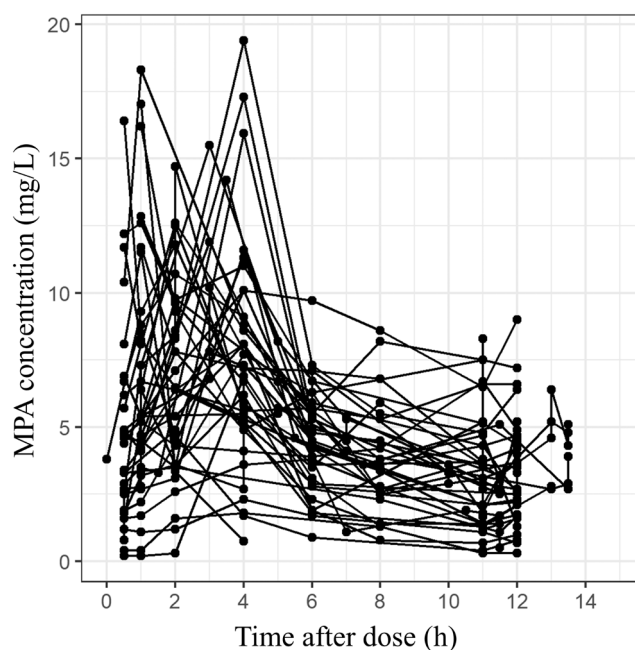

FIGURE 1 Observed mycophenolic acid concentration versus time after dose based on individual patient data.

incorporating sequential zero- and first-order absorption with lag time and first-order elimination, was selected as the final candidate popPK model. The parameters of this model included the apparent clearance (CL/*F*), apparent central volume of distribution (VC/*F*), apparent intercompartmental clearance (*Q*/*F*), apparent peripheral volume of distribution (VP/*F*), absorption half-life (TABS), lag time (TLAG), and duration of zero-order absorption (D1).
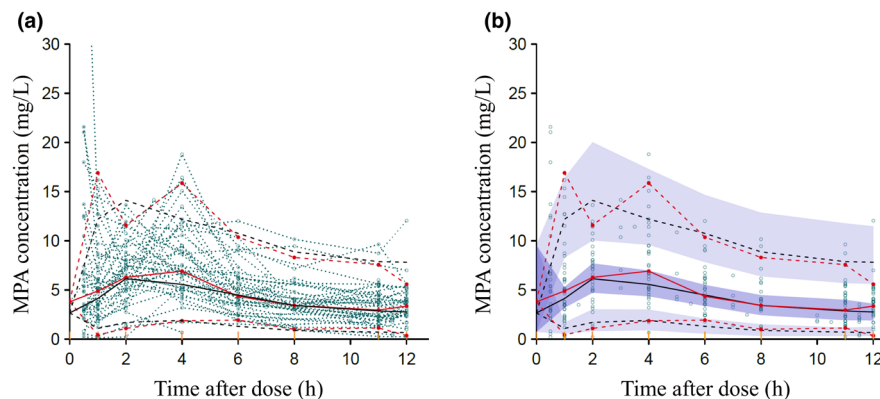
FIGURE 2 Prediction-corrected visual predictive check of mycophenolic acid concentration versus time after dose based on final population pharmacokinetic model parameters of mycophenolic acid. (a) Green dotted lines and circles connect the observed data points for each participant. Red and black lines represent the median (solid) and 90% prediction intervals (dashed) of the observed data and predicted data, respectively. (b) Green circles represent the observed data. Red and black lines represent the median (solid) and 90% prediction intervals (dashed) of the observed data and predicted data, respectively. The shaded areas represent the 95% confidence intervals for the median and 90% prediction intervals.

Covariate model

F_{fat} was included in the NFM calculation as a factor accounting for the influence of FAT. The OFV with estimated F_{fat} values for CL/F, VC/F, VP/F, and Q/F did not differ significantly from those with F_{fat} set at 1.

In the covariate analysis, RF was selected as a significant covariate for CL_{renal}/F and PTD was selected as a significant covariate for relative bioavailability (F1) (Table S1). The final model PK parameters are given by the following Equation (8). The NM-TRAN control stream is shown in Appendix S1.

$$CL/F\,(\text{L/h}) = (7.56 + 11.6 \times RF) \times \left(\frac{TBW}{TBW_{std}}\right)^{\frac{3}{4}}$$

$$VC/F\,(\text{L}) = 104.0 \times \left(\frac{TBW}{TBW_{std}}\right)$$

$$Q/F\,(\text{L/h}) = 17.3 \times \left(\frac{TBW}{TBW_{std}}\right)^{\frac{3}{4}}$$

$$VP/F\,(\text{L}) = 169.0 \times \left(\frac{TBW}{TBW_{std}}\right)$$

$$\text{ka}\,(\text{h}^{-1}) = \frac{0.693}{0.0453}$$

$$\text{ALAG1}\,(\text{L}) = 0.283$$

$$D1\,(\text{L}) = 1.95$$

$$F_{PTD} = e^{0.956 \times \frac{PTD}{PTD_{max}}} \tag{8}$$

Model evaluation and validation

The GOF plots obtained from the final PK model are shown in Figure S2. The predicted concentrations agreed well with the observed concentrations, and the distribution of the plots was near the trend line $y = x$. There was no trend in the distribution of CWRES over the population prediction and time after dose; most CWRESs were within 3.

The results of the pcVPC are shown in Figure 2. The median of the observed values closely matched the predicted values. The 90% quantiles of the observed values were within 95% confidence intervals of the predicted values.

The final parameter estimates and results of the bootstrap method are presented in Table 2. Parameter estimates obtained from the final popPK model matched the mean and median of the parameter estimates derived from the bootstrap results and were within the 95% confidence intervals of the bootstrap results.

Simulation

The relationship between PTD and MPA AUC0–12 of MMF 500 mg administered to patients with different RF is shown in Figure 3. MPA AUC0–12 increased with increasing PTD and decreasing RF. During the early post-transplantation period, the recommended dose was 500 mg every 12 h for patients with a CLcr of 25 mL/min, 750 mg every 12 h for patients with a CLcr of 50 mL/min, and 1000 mg every 12 h for patients with a CLcr of 75 and 100 mL/min.

TABLE 2 Summary of parameter estimates and bootstrap results of the final model.

| Parameters | Unit | Final model estimate | Bootstrap sample estimates ($n = 200$) | | | | |
| | | | Mean | Median | 95% CI[a] | | %RSE |
					Lower 2.5%	Upper 97.5%	
Population mean							
Apparent nonrenal clearance	L/h	7.56	7.87	7.52	5.36	13.53	25.4
Apparent renal clearance	L/h	11.6	11.3	11.6	3.8	18.0	30.0
Apparent central volume of distribution	L	104.0	100.8	100.0	68.1	143.0	18.9
Apparent intercompartment clearance	L/h	17.3	19.3	18.3	10.1	35.2	31.3
Apparent peripheral volume of distribution	L	169.0	279.0	195.0	68.7	1060.0	89.1
Absorption half-life	h	0.0453	0.0485	0.0443	0.0102	0.1285	67.6
Lag time	h	0.283	0.292	0.286	0.145	0.475	26.4
Duration of zero-order absorption	h	1.95	1.78	1.77	1.26	2.27	15.7
Relative bioavailability	–	1 fixed	–	–	–	–	–
Effect of posttransplantation day on relative bioavailability	–	0.956	1.010	0.970	0.529	1.773	26.8
F_{fat} for clearance	–	1 fixed	–	–	–	–	–
F_{fat} for volume of distribution	–	1 fixed	–	–	–	–	–
Between-subject variability							
Apparent clearance	CV%	42.8	40.0	41.2	14.1	58.8	28.8
Apparent central volume of distribution	CV%	58.1	61.1	60.7	33.0	87.4	23.2
Apparent intercompartment clearance	CV%	0 fixed	–	–	–	–	–
Apparent peripheral volume of distribution	CV%	0 fixed	–	–	–	–	–
Absorption half-life	CV%	73.1	105.4	76.0	64.7	301.7	65.8
Lag time	CV%	121.7	121.7	119.6	85.4	174.8	22.5
Duration of zero-order absorption	CV%	90.8	88.8	88.2	68.1	113.6	13.4
Relative bioavailability	CV%	18.0	17.7	17.2	2.6	37.7	52.3
Residual unidentified variability							
Proportional residual unidentified variability	CV%	28.3	26.9	27.0	22.9	30.0	7.1
Additive residual unidentified variability	mg/L	0.0634	0.0874	0.0639	0.0138	0.3053	79.0

Abbreviations: CI, confidence interval; CV, coefficient of variance; RSE, relative standard error.

[a]95% CI was estimated from 2.5 to 97.5 percentile of the bootstrap sample estimates.

DISCUSSION

In this study, a popPK model of MPA was developed for patients with renal transplants. An EHC model was not selected; instead, the PK of MPA was adequately described using a two-compartment model with sequential zero- and first-order absorption following a lag time. Given that after oral administration MMF is rapidly converted to MPA in the stomach and MMF can hardly be detected in plasma,[3] an MMF dose was adjusted to MPA using their molecular weight. The predictive performance and robustness of the developed popPK model were demonstrated through the pcVPC and bootstrap results.

This is the first study to explore multiple absorption models of MPA, demonstrating that sequential zero- and first-order absorption best describes MPA absorption in patients with renal transplants. Although various absorption models have been reported, such as zero-order absorption,[12,13] parallel zero- and first-order absorption,[14] parallel first-order absorption,[15] and transit-compartment absorption,[16–18] these were not selected in this study. One reason for selecting the sequential zero- and first-order absorption model was the variability observed in the absorption process in this study. In some patients, MPA was absorbed slowly, exhibiting a delayed t_{max} (Figure 1). To explain this variability, three
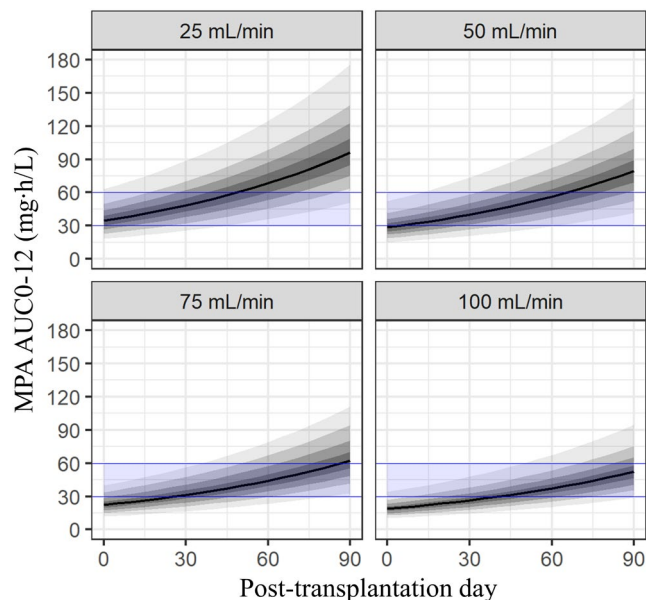
FIGURE 3 Predicted time course of area under the concentration-time curve at 0–12 h (AUC0–12) of mycophenolic acid (MPA) following renal transplant. Predicted time course of AUC0–12 of MPA based on the final population pharmacokinetic model parameters in patients with different renal functions (creatinine clearance 25, 50, 75, and 100 mL/min). Solid line represents the median values of predicted MPA concentrations, while gray areas represent 10%–90% intervals of predictions. Blue-shaded areas represent the target MPA AUC0–12 (30–60 mg h/L). The dosing regimen of 500 mg MMF every 12 h was assumed.

parameters were used: the duration of zero-order absorption, absorption half-life, and lag time. The estimated BSV for these absorption parameters was relatively large (Table 2). Incorporating the variability of the absorption process using a sequential zero- and first-order absorption model may account for the large variability in the PK of MPA observed in this study.

The physicochemical properties of MPA also support the selection of this model. MMF exhibits pH-dependent solubility and is classified as a Class II compound in the Biopharmaceutical Classification System (BCS).[35] In agreement with the findings of this study, previous studies have reported that a sequential zero- and first-order absorption model is appropriate for other BCS Class II compounds.[36–38] Further studies are required to elucidate why this model is suitable for BCS Class II compounds.

In the covariate analysis, using a stepwise approach, we comprehensively incorporated each covariate into the final candidate model one by one and selected covariates that significantly changed OFV. The TBW, RF, and PTD were included as covariates affecting the PK of MPA. The NFM estimation of F_{fat} was tested; however, F_{fat} did not significantly differ from 1, indicating that the PK of MPA was influenced by TBW. After oral administration

of radiolabeled MMF, approximately 93% of the dose was excreted in the urine.[4] RF is considered crucial in the PK of MPA and was included as a covariate. Although the effects of PTD on CL/F and VC/F have been reported previously,[25,39] in this study, PTD was selected as a covariate for relative bioavailability. The relative bioavailability increased over PTD and was predicted to be 2.8-fold higher at 90 days posttransplantation than on the day of transplantation. These results were consistent with those of previous reports showing a time-dependent increase in MPA exposure.[25,40] This could be attributed to an alteration of the gut environment following renal transplantation. The differences in gut environment between healthy individuals and patients with chronic kidney disease and the alteration in gut microbiota profile following kidney transplantation are well established.[41,42] These changes, in turn, may increase drug absorption, potentially resulting in increased MPA exposure.

In this study, tacrolimus and prednisone were concomitantly administered in some patients. Kim et al.[43] reported that tacrolimus did not change the PK parameters of MPA and its metabolites. On the contrary, a previous study reported that glucocorticoids induced the hepatic uridine 5′-diphospho-glucuronosyltransferase (UGT) activity and decreased the bioavailability of MPA.[44] Cattaneo et al.[44] reported that discontinuation of glucocorticoids resulted in higher MPA exposure and lower MPAG trough levels. With the concomitant use of glucocorticoids, the concentration of MPAG increases, and the proportion of EHC of MPAG may increase, potentially resulting in a clear second peak. However, in this study, the number of patients exhibiting a clear second peak was limited, suggesting that the PKs of MPA did not change significantly with the concomitant use of prednisone. Additionally, the inclusion of tacrolimus and prednisone as a covariate of CL/F and VC/F in the final model did not show significant improvement of OFV (data not shown). Tacrolimus and prednisone are unlikely to affect the PKs of MPA in this study.

The recommended target AUC for MPA AUC0–12 during MMF administration is 30–60 mg h/L.[3,5] In this study, a recommended individualized dose based on the PTD and RF was proposed by simulating the MPA AUC0–12. The simulation results indicated that achieving the target AUC0–12 requires reducing the MMF dose with an increase in PTD and a decreased RF. The recommended dose was within the dose stated in the package insert of Cellcept® in Japan, USA, and Europe.[45–47] MPA exposure is approximately 75% higher in patients with severe renal impairment than in healthy individuals.[48] Moreover, doses of MMF greater than 1 g twice a day should be avoided, as stated in the package insert of Cellcept®.[46,47] The recommended dose in patients with

severe renal impairment (CLcr = 25 mL/min/70 kg) in this study was also within the dose stated in the package insert of Cellcept®. Thus, the developed popPK model can provide useful information on individualized doses of MMF based on PTD and RF.

This study had some limitations. First, owing to the sample size and variability of the PK of MPA, the number of patients exhibiting a clear second peak was limited. This may explain why an EHC model was not adopted in this study. Previous study has indicated a six-fold interindividual variability in the contribution of EHC to AUC.[4] Without EHC, it is difficult to predict the MPA exposure, including the contribution of EHC, and the increase in exposure due to EHC is not predicted. MPA exposure could be underestimated, leading to an unexpected rise in MMF dose. Further studies using a larger dataset and more cases showing a clear second peak are necessary to assess the contribution of absorption delay and the EHC process to the PK of MPA. Second, unbound MPA and MPAG were excluded due to data unavailability. Given that free drugs contribute to pharmacological action, it is desirable to include unbound MPA concentrations to predict individual clinical responses. The MPAG is involved in EHC.[1] Several popPK models with unbound MPA and the EHC of MPAG have been reported.[13,16,20–23] A more mechanistic model could be developed in the future by incorporating both unbound MPA and MPAG. Finally, a popPK model was developed using data collected within 3 months of transplantation. Data collected beyond this timeframe were not used for model development because of its limited availability. Previous reports[49,50] suggest that MPA exposure stabilizes 3 months after transplantation. The development of a popPK model using data collected beyond 3 months posttransplantation is necessary for MMF, which is continuously administered for an extended period.

In the present study, the PK of MPA was adequately described using a two-compartment model incorporating sequential zero- and first-order absorption with lag time. Individual dosing regimens with a high probability of achieving the target MPA AUC0–12 were predicted using the popPK model. The popPK model can be used to propose individual dosing regimens for patients undergoing renal transplantation.

AUTHOR CONTRIBUTIONS

Y.S. wrote the manuscript. Y.S., N.M., T.A., C.O., C.H., S.I., H.T., T.K., and Y.T. designed the research. Y.S., N.M., T.A., C.O., T.K., and Y.T. performed the research. Y.S., T.A., C.O., and Y.T. analyzed the data.

FUNDING INFORMATION

CONFLICT OF INTEREST STATEMENT

DATA AVAILABILITY STATEMENT

ORCID

Yuki Suzuki https://orcid.org/0009-0008-9283-9802
Takahiko Aoyama https://orcid.org/0000-0001-6111-8537
Chika Ogami https://orcid.org/0000-0002-2493-9616
Chihiro Hasegawa https://orcid.org/0000-0003-1473-5617
Yasuhiro Tsuji https://orcid.org/0000-0002-7967-2947

REFERENCES

1. Staatz CE, Tett SE. Clinical pharmacokinetics and pharmacodynamics of mycophenolate in solid organ transplant recipients. *Clin Pharmacokinet*. 2007;46(1):13-58. doi:10.2165/00003088-200746010-00002

2. van Sandwijk MS, Bemelman FJ, Ten Berge IJM. Immunosuppressive drugs after solid organ transplantation. *Neth J Med*. 2013;71(6):281-289.

3. Bergan S, Brunet M, Hesselink DA, et al. Personalized therapy for mycophenolate: consensus report by the International Association of Therapeutic Drug Monitoring and Clinical Toxicology. *Ther Drug Monit*. 2021;43(2):150-200. doi:10.1097/FTD.0000000000000871

4. Bullingham RE, Nicholls AJ, Kamm BR. Clinical pharmacokinetics of mycophenolate mofetil. *Clin Pharmacokinet*. 1998;34(6):429-455. doi:10.2165/00003088-199834060-00002

5. Kuypers DRJ, Le Meur Y, Cantarovich M, et al. Consensus report on therapeutic drug monitoring of mycophenolic acid in solid organ transplantation. *Clin J Am Soc Nephrol*. 2010;5:341-358. doi:10.2215/CJN.07111009

6. Staatz CE, Tett SE. Pharmacology and toxicology of mycophenolate in organ transplant recipients: an update. *Arch Toxicol*. 2014;88(7):1351-1389. doi:10.1007/s00204-014-1247-1

7. Kiang TKL, Ensom MHH. Exposure-toxicity relationships of mycophenolic acid in adult kidney transplant patients. *Clin Pharmacokinet*. 2019;58(12):1533-1552. doi:10.1007/s40262-019-00802-z

8. Shum B, Duffull SB, Taylor PJ, Tett SE. Population pharmacokinetic analysis of mycophenolic acid in renal transplant recipients following oral administration of mycophenolate mofetil. *Br J Clin Pharmacol*. 2003;56(2):188-197. doi:10.1046/j.1365-2125.2003.01863.x

9. Staatz CE, Duffull SB, Kiberd B, Fraser AD, Tett SE. Population pharmacokinetics of mycophenolic acid during the first week after renal transplantation. *Eur J Clin Pharmacol*. 2005;61(7):507-516. doi:10.1007/s00228-005-0927-4

10. Sherwin CMT, Fukuda T, Brunner HI, Goebel J, Vinks AA. The evolution of population pharmacokinetic models to describe

the enterohepatic recycling of mycophenolic acid in solid organ transplantation and autoimmune disease. *Clin Pharmacokinet*. 2011;50(1):1-24. doi:10.2165/11536640-000000000-00000

11. Kiang TKL, Ensom MHH. Population pharmacokinetics of mycophenolic acid: an update. *Clin Pharmacokinet*. 2018;57(5):547-558. doi:10.1007/s40262-017-0593-6

12. Le Guellec C, Bourgoin H, Büchler M, et al. Population pharmacokinetics and Bayesian estimation of mycophenolic acid concentrations in stable renal transplant patients. *Clin Pharmacokinet*. 2004;43(4):253-266. doi:10.2165/00003088-200443040-00004

13. Riglet F, Bertrand J, Barrail-Tran A, et al. Population pharmacokinetic model of plasma and cellular mycophenolic acid in kidney transplant patients from the CIMTRE study. *Drugs R D*. 2020;20(4):331-342. doi:10.1007/s40268-020-00319-y

14. Wang G, Ye Q, Huang Y, Xu H, Li Z. Population pharmacokinetics of enteric-coated mycophenolate sodium in children after renal transplantation and initial dosage recommendation based on body surface area. *Comput Math Methods Med*. 2022;2022:1881176. doi:10.1155/2022/1881176

15. de Winter BCM, Neumann I, van Hest RM, van Gelder T, Mathot RAA. Limited sampling strategies for therapeutic drug monitoring of mycophenolate mofetil therapy in patients with autoimmune disease. *Ther Drug Monit*. 2009;31(3):382-390. doi:10.1097/FTD.0b013e3181a23f1a

16. Sherwin CMT, Sagcal-Gironella ACP, Fukuda T, Brunner HI, Vinks AA. Development of population PK model with enterohepatic circulation for mycophenolic acid in patients with childhood-onset systemic lupus erythematosus. *Br J Clin Pharmacol*. 2012;73(5):727-740. doi:10.1111/j.1365-2125.2011.04140.x

17. Dong M, Fukuda T, Cox S, et al. Population pharmacokinetic-pharmacodynamic modelling of mycophenolic acid in paediatric renal transplant recipients in the early post-transplant period. *Br J Clin Pharmacol*. 2014;78(5):1102-1112. doi:10.1111/bcp.12426

18. Mizaki T, Nobata H, Banno S, et al. Population pharmacokinetics and limited sampling strategy for therapeutic drug monitoring of mycophenolate mofetil in Japanese patients with lupus nephritis. *J Pharm Health Care Sci*. 2023;9(1):1. doi:10.1186/s40780-022-00271-w

19. Funaki T. Enterohepatic circulation model for population pharmacokinetic analysis. *J Pharm Pharmacol*. 1999;51(10):1143-1148. doi:10.1211/0022357991776831

20. Sheng C, Zhao Q, Niu W, Qiu X, Zhang M, Jiao Z. Effect of protein binding on exposure of unbound and total mycophenolic acid: a population pharmacokinetic analysis in Chinese adult kidney transplant recipients. *Front Pharmacol*. 2020;11:340. doi:10.3389/fphar.2020.00340

21. Yau WP, Vathsala A, Lou HX, Zhou S, Chan E. Mechanism-based enterohepatic circulation model of mycophenolic acid and its glucuronide metabolite: assessment of impact of cyclosporine dose in asian renal transplant patients. *J Clin Pharmacol*. 2009;49(6):684-699. doi:10.1177/0091270009332813

22. Okour M, Jacobson PA, Ahmed MA, Israni AK, Brundage RC. Mycophenolic acid and its metabolites in kidney transplant recipients: a semimechanistic enterohepatic circulation model to improve estimating exposure. *J Clin Pharmacol*. 2018;58(5):628-639. doi:10.1002/jcph.1064

23. De Winter BCM, Van Gelder T, Sombogaard F, Shaw LM, Van Hest RM, Mathot RAA. Pharmacokinetic role of protein binding of mycophenolic acid and its glucuronide metabolite in renal transplant recipients. *J Pharmacokinet Pharmacodyn*. 2009;36(6):541-564. doi:10.1007/s10928-009-9136-6

24. Zhang HX, Sheng CC, Liu LS, et al. Systematic external evaluation of published population pharmacokinetic models of mycophenolate mofetil in adult kidney transplant recipients co-administered with tacrolimus. *Br J Clin Pharmacol*. 2019;85(4):746-761. doi:10.1111/bcp.13850

25. Wang P, Xie H, Zhang Q, et al. Population pharmacokinetics of mycophenolic acid in renal transplant patients: a comparison of the early and stable posttransplant stages. *Front Pharmacol*. 2022;13:859351. doi:10.3389/fphar.2022.859351

26. Woillard JB, Debord J, Marquet P. Comment on "population pharmacokinetics of mycophenolic acid: an update". *Clin Pharmacokinet*. 2018;57(9):1211-1213. doi:10.1007/s40262-018-0687-9

27. Cockcroft DW, Gault MH. Prediction of creatinine clearance from serum creatinine. *Nephron*. 1976;16(1):31-41. doi:10.1159/000180580

28. Goulooze SC, Krekels EHJ, Hankemeier T, Knibbe CAJ. Covariates in pharmacometric repeated time-to-event models: old and new (pre)selection tools. *AAPS J*. 2019;21(1):11. doi:10.1208/s12248-018-0278-6

29. Rousseau A, Léger F, Le Meur Y, et al. Population pharmacokinetic modeling of oral cyclosporin using NONMEM: comparison of absorption pharmacokinetic models and design of a Bayesian estimator. *Ther Drug Monit*. 2004;26(1):23-30. doi:10.1097/00007691-200402000-00006

30. Savic RM, Jonker DM, Kerbusch T, Karlsson MO. Implementation of a transit compartment model for describing drug absorption in pharmacokinetic studies. *J Pharmacokinet Pharmacodyn*. 2007;34(5):711-726. doi:10.1007/s10928-007-9066-0

31. Holford NHG, Anderson BJ. Allometric size: the scientific theory and extension to normal fat mass. *Eur J Pharm Sci*. 2017;109:S59-S64. doi:10.1016/j.ejps.2017.05.056

32. Anderson BJ, Holford NHG. Mechanistic basis of using body size and maturation to predict clearance in humans. *Drug Metab Pharmacokinet*. 2009;24(1):25-36. doi:10.2133/dmpk.24.25

33. Holford NHG, Anderson BJ. Why standards are useful for predicting doses. *Br J Clin Pharmacol*. 2017;83(4):685-687. doi:10.1111/bcp.13230

34. Holford N, Heo YA, Anderson B. A pharmacokinetic standard for babies and adults. *J Pharm Sci*. 2013;102(9):2941-2952. doi:10.1002/jps.23574

35. Scheubel E, Adamy L, Cardot JM. Mycophenolate mofetil: use of a simple dissolution technique to assess generic formulation differences. *Dissolut Technol*. 2012;19(1):52-58. doi:10.14227/DT190112P52

36. Robarge JD, Metzger IF, Lu J, et al. Population pharmacokinetic modeling to estimate the contributions of genetic and nongenetic factors to efavirenz disposition. *Antimicrob Agents Chemother*. 2017;61(1):e01813-16. doi:10.1128/AAC.01813-16

37. González-Sales M, Djebli N, Meneses-Lorente G, et al. Population pharmacokinetic analysis of entrectinib in pediatric and adult patients with advanced/metastatic solid tumors: support of new drug application submission. *Cancer Chemother Pharmacol*. 2021;88(6):997-1007. doi:10.1007/s00280-021-04353-8

38. Li J, Karlsson MO, Brahmer J, et al. CYP3A phenotyping approach to predict systemic exposure to EGFR tyrosine kinase inhibitors. *J Natl Cancer Inst.* 2006;98(23):1714-1723. doi:10.1093/jnci/djj466

39. Rexiti K, Jiang X, Kong Y, et al. Population pharmacokinetics of mycophenolic acid and dose optimisation in adult Chinese kidney transplant recipients. *Xenobiotica.* 2023;53(10–11):603-612. doi:10.1080/00498254.2023.2287168

40. Jeong H, Kaplan B. Therapeutic monitoring of mycophenolate mofetil. *Clin J Am Soc Nephrol.* 2007;2(1):184-191. doi:10.2215/CJN.02860806

41. Campbell PM, Humphreys GJ, Summers AM, et al. Does the microbiome affect the outcome of renal transplantation? *Front Cell Infect Microbiol.* 2020;10:558644. doi:10.3389/fcimb.2020.558644

42. Lee JR, Muthukumar T, Dadhania D, et al. Gut microbial community structure and complications after kidney transplantation: a pilot study. *Transplantation.* 2014;98(7):697-705. doi:10.1097/TP.0000000000000370

43. Kim JH, Han N, Kim MG, et al. Increased exposure of tacrolimus by co-administered mycophenolate mofetil: population pharmacokinetic analysis in healthy volunteers. *Sci Rep.* 2018;8(1):1687. doi:10.1038/s41598-018-20071-3

44. Cattaneo D, Perico N, Gaspari F, Gotti E, Remuzzi G. Glucocorticoids interfere with mycophenolate mofetil bioavailability in kidney transplantation. *Kidney Int.* 2002;62(3):1060-1067. doi:10.1046/j.1523-1755.2002.00531.x

45. Ministry of Health Labor and Welfare. CELLCEPT (mycophenolate mofetil) PRESCRIBING INFORMATION in Japanese. Accessed August 13, 2024. https://www.pmda.go.jp/PmdaSearch/iyakuDetail/ResultDataSetPDF/450045_3999017B1025_1_14

46. US Food and Drug Administration. CELLCEPT (mycophenolate mofetil) PRESCRIBING INFORMATION. Accessed August 13, 2024. https://www.accessdata.fda.gov/drugsatfda_docs/label/2022/050722s050,050723s050,050758s048,050759s055lbl.pdf

47. European Medicines Agency. CellCept (mycophenolate mofetil) SUMMARY OF PRODUCT CHARACTERISTICS. Accessed August 13, 2024. https://www.ema.europa.eu/en/documents/product-information/cellcept-epar-product-information_en.pdf

48. Johnson HJ, Swan SK, Heim-Duthoy KL, Nicholls AJ, Tsina I, Tarnowski T. The pharmacokinetics of a single oral dose of mycophenolate mofetil in patients with varying degrees of renal function. *Clin Pharmacol Ther.* 1998;63(5):512-518. doi:10.1016/S0009-9236(98)90102-3

49. Weber LT, Shipkova M, Armstrong VW, et al. Comparison of the emit immunoassay with HPLC for therapeutic drug monitoring of mycophenolic acid in pediatric renal-transplant recipients on mycophenolate mofetil therapy. *Clin Chem.* 2002;48(3):517-525.

50. Le Meur Y, Büchler M, Thierry A, et al. Individualized mycophenolate mofetil dosing based on drug exposure significantly improves patient outcomes after renal transplantation. *Am J Transplant.* 2007;7(11):2496-2503. doi:10.1111/j.1600-6143.2007.01983.x

SUPPORTING INFORMATION

Additional supporting information can be found online in the Supporting Information section at the end of this article.